Shape instability on swelling of a stretched nematic elastomer filament

N. Cheewaruangroj and E. M. Terentjev
Cavendish Laboratory, University of Cambridge, JJ Thomson Avenue, Cambridge CB3 0HE, U.K.
(Dated: September 18, 2015)

Liquid crystalline elastomers combine the ordering properties of liquid crystals with elasticity of cross-linked polymer networks. In monodomain (permanently aligned) elastomers, altering the orientational (nematic) order causes changes in the equilibrium sample length, which is the basis of the famous effect of large-amplitude reversible mechanical actuation. The stimulus for this effect could be a change in temperature, or illumination by light in photo-sensitized elastomers, but equally the nematic order changes by mixing with a solvent. This work theoretically investigates a competition between the spontaneous contraction on swelling of a monodomain nematic elastomer and the externally imposed stretching. We find that this competition leads to bistability in the system and allows a two-phase separation between a nematic state with lower swelling and an isotropic state with higher solvent concentration. We calculated the conditions in which the instability occurs as well as the mechanical and geometric parameters of equilibrium states. Being able to predict how this instability arises will provide opportunities for exploiting nematic elastomer filaments.

PACS numbers: 61.30.Vx, 83.80.Va, 61.25.hp

I. INTRODUCTION

Liquid crystalline elastomers (LCEs) are cross-linked rubber-elastic polymers, which also have properties of liquid crystals arising from mesogenic molecules that are a part of the polymer chains. They combine elasticity of elastomers with orientation ordering of liquid crystals, making them special and distinct from other elastic materials, a concept originally introduced by de Gennes in 1975 [1]. Changing the average order parameter of the mesogenic units affects the equilibrium shape of the LCEs. This reversible shape variation was predicted by Warner [2] and Khokhlov [3] and first achieved in experiment by Finkelmann [4] after the uniformly aligned (monodomain) LCE materials were developed. As a result, LCEs can be used for their mechanical actuation from applying heat [5], light [6] or solvents [7]. Another application is to use their birefringence properties, which can be manipulated mechanically [8]. In some liquid crystalline phases, other than simple nematic, they also have photonic structures with band gaps and exhibit mechanically tunable optical effects, which can be very useful in display devices [9].

Mechanical actuation in nematic LCEs arises from the coupling of the rubber elasticity and the order parameter. As the order parameter changes, the elastic free energy evolves and so does the spontaneous expansion of the material. Similar to any phase transitions, the order parameter $Q(T)$ depends on the temperature for T below the critical temperature, T_c. This is observed in the experiment as a change in the spontaneous uniaxial expansion as the temperature drops [5]. The changes in the extension can be very large — up to 500% in the record experiment [10], while a reversible uniaxial extension by 30-60% is a commonplace in nematic LCEs. The same effect could be observed with light as a stimulus, instead of heat, either due to an effect of photoisomerizationthat can change their order parameter and shift the phase transition [11], or by simply converting light to local heat in the network and observing the effectively thermal effect [12]. Adding impurities (e.g. isotropic solvent) has the same effect as photo-isomerization. The critical temperature of isotropic-nematic transition decreases linearly with the impurity concentration and hence changes the order parameter [13]. This will be discussed in more details in section II.

Using nematic LCEs as actuators can be difficult in practice because of the domain boundaries that persist even though the director in each domain aligns in the same direction [14]; this is an especially well-known issue with monodomain LCEs prepared by the 'two-step crosslinking' method of Finkelmann [4]. One way of improving the nematic alignment and thus enhancing the actuation is by using aligned fibers. Shape-memory fibers have many real-world applications from textiles to biomimetic fibers [10]. Several groups were successful in producing such fibers in the lab [15, 16]. The shape-memory response of the nematic LCE fibers is very strong compared to other types of materials, which is due to a higher degree of alignment in a fiber that was formed under high tension; the actuation response time is also short as the fibers can be made very thin and exchange heat faster.

Polymer gels have been studied intensively because of their many applications [17]. They can be made of thin fibers, which can be useful for biological materials such as artificial muscles [18]. Swelling of ordinary isotropic gels under deformation has been recently studied for both good and poor solvents surrounding the swollen network [19]; one of the fundamental results is that a gel in a bath of good solvent takes in more solvent (i.e. increases its volume) under tensile deformation. Gels created from nematic LCEs have an additional internal degree of freedom, the nematic order, which is coupled to both solvent intake and the elastic deformation of the network. One expects dramatic effects on swelling of monodomain

(aligned) LCEs because of their strong mechanical actuation in response to the changing order parameter, and indeed theories have been developed to describe these effects [20, 21].

In this paper we want to extend this theoretical analysis to a situation when an elastomer sample under imposed tensile strain is swelling in a solvent. Although the theory we develop is not explicitly linked to a thin fiber shape of samples, we would like to have this geometry in mind – especially to avoid complicate issues of inhomogeneous swelling and gradients (of solvent, of strain, and of the nematic order) across the sample cross-section when it is subjected to a uniaxial extension. It also helps the speed of solvent transfer across the thin sample. Under a large deformation, gels often undergo instabilities. Necking is one of the examples of such instabilities, where the material splits into the necking region of plastic deformation and the normal region with different cross-sectional areas. We need to consider possibilities of having instabilities from deforming stretched LCE gels as well.

The effects of stretching and solvent mixing compete against each other. For good solvents, mixing would cause the elastomer to swell. However, this would stretch the elastomer and so increases the elastic free energy. The swollen will be limited by these two factors. Complication arises from the phase transition induced by the solvents. At highly swollen state, the elastomer could become isotropic and responses differently to the stretching. This could allow the elastomer to exist in two different phases, which could cause the formation of the solvent rich 'pocket' coexisting with a less swollen still-nematic (i.e. naturally extended) region of the sample. The aim of this theoretical work is to find a description of such an instability as well as calculating the size of each region.

II. BACKGROUND THEORY

Liquid crystal elastomer

The nematic liquid crystalline order parameter is defined as the orientational average over the typically rod-like mesogenic units: $Q = \frac{3}{2}(\langle\cos^2\theta\rangle - \frac{1}{3})$, where θ is the angle between each uniaxially anisotropic (mesogenic) molecule and the average director axis. The polymer backbones couple to the mesogens and change their structure depending on the order parameter. In our case, the structure is uniaxial with the nematic director along the stretching axis (z-direction). This is described by step lengths, $l_\perp$ and $l_\parallel$, perpendicular and parallel to the nematic director. In the isotropic phase, we have $l_\perp = l_\parallel = a$, where a is the isotropic step length. On the other hand, in the nematic phase, they are different and depend on the order parameter by [22]:

$$l_\perp = a(1-Q), \quad l_\parallel = a(1+2Q). \tag{1}$$

These expressions appear strongly model dependent (indeed, originally derived for a freely-jointed rod model of nematic polymer chains). However, the qualitative relation – that $l_\parallel$ increases with the growth of nematic order while $l_\perp$ decreases, in a ratio 2:1 – is quite universal, and in practice there have been many measurements of these parameters in different materials, more or less confirming the Eq. 1 in most side-chain LCEs (in the exceptional and more rare case of main-chain LCE the dependence $l_\parallel(Q)$ is much sharper [23]).

The elastic free energy of a nematic LCE is given by the 'Trace formula' [24, 25]

$$F_{\rm el} = \frac{N_{\rm x}}{2} k_{\rm B}T \left(\mathrm{Tr}\left[\underline{\underline{l}}_0 \cdot \underline{\underline{\lambda}}^T \cdot \underline{\underline{l}}^{-1} \cdot \underline{\underline{\lambda}}\right] - \ln \frac{\det \underline{\underline{l}}_0}{\det \underline{\underline{l}}} \right), \tag{2}$$

where $N_{\rm x}$ is the number of cross-links in the elastomer. Note that we are writing the full, extensive form of the free energy, in contrast to typical literature expressions giving the intensive energy density in this context. The reason is that we shall need to account for the total amount of solvent in different parts of the sample, and our analysis goes better with full expressions. However, to link with the traditionally used format, we define an intensive parameter: the crosslinking ratio, ν, as the number of cross-links per monomer ($1/\nu$ gives an average number of monomers between crosslinks on a network strand). This gives $N_{\rm x} = \nu N_{\rm p}$, where $N_{\rm p}$ is the total number of monomer 'particles' in the cross-linked polymer network.

The matrix $\underline{\underline{l}}$ in Eq.(2) describes step lengths that a chain random walk makes in each direction, which in the uniaxial case can be written in principal axes ('parallel' meaning along the nematic director):

$$\underline{\underline{l}} = \begin{pmatrix} l_\perp & 0 & 0 \\ 0 & l_\perp & 0 \\ 0 & 0 & l_\parallel \end{pmatrix}. \tag{3}$$

The subscript ..$_0$ denotes the quantities at the initial state before the deformation or swelling is applied to the sample. The deformation tensor is $\lambda_{ij} = 1 + \epsilon_{ij}$, where ϵ_{ij} is the strain. For dry elastomers the volume has to be conserved, which imposes a constraint on the principal extensions: $\lambda_x\lambda_y\lambda_z = 1$. Hence, for a uniaxial deformation imposed along the z-axis, $\lambda_x = \lambda_y = 1/\sqrt{\lambda_z} \equiv 1/\sqrt{\lambda}$. Putting everything together and minimizing $F_{\rm el}$ with respect to λ, the spontaneous extension that occurs due to the underlying nematic order can be calculated as [24]

$$\lambda_m = \left(\frac{l_\parallel l_{\perp 0}}{l_{\parallel 0} l_\perp}\right)^{1/3} = \left(\frac{r}{r_0}\right)^{1/3}, \tag{4}$$

where $r \equiv l_\parallel/l_\perp$ is a non-dimensional ratio that characterizes the uniaxial anisotropy in the polymer backbone. Substituting (1) in (4), λ_m can be calculated as a function of the order parameter, $Q(T)$. Increasing Q (e.g. by lowering temperature) increases the ratio r and so the length of the elastomer is larger [2, 3]. This is the modern format of the basic theory behind the effect of reversible thermal actuation of monodomain LCEs.

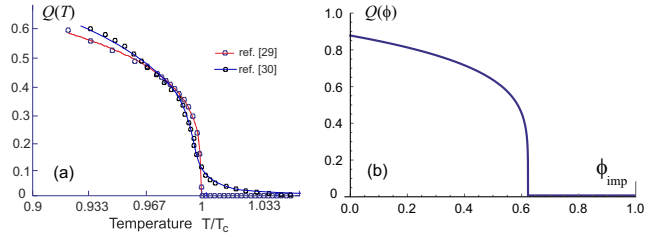

FIG. 1: [Color online] (a) The nematic order parameter Q as a function of scaled temperature T/T_c, the data from two recent experimental studies highlighting the critical and supercritical cases. (b) The order parameter plotted against solvent concentration, labelled here as $\phi_{\rm imp}$, using the parametrization in Eqs. (5) and (6).

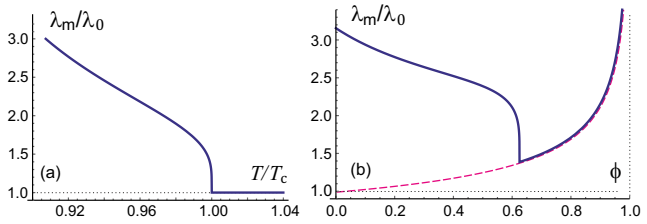

FIG. 2: [Color online] (a) The spontaneous extension of a uniaxial nematic elastomer along its director as a function of temperature, Eqs. (4) and (5). (b) The spontaneous extension in the case when the nematic order is reduced by the added solvent of volume fraction ϕ, Eq. (7). The dashed line is the isotropic $\lambda = (1-\phi)^{-1/3}$.

Instead of solving a complicated problem of weak first order transition in an elastomer with mechanical-orientational coupling (which is the contents of [22]), we can simply use the results from experiments [26, 27] to parametrize the temperature dependence of the order parameter $Q(T)$:

$$Q = \begin{cases} Q_0|T-T_{\rm c}|^{\xi} & \text{for } T \le T_c \\ 0 & \text{for } T > T_c \end{cases}, \qquad (5)$$

where Q_0 is a constant, T_c is the isotropic-nematic transition temperature, and the exponent $\xi \approx 0.2$. One may question why in practice there appears to be a critical point at T_c while the nematic transition is a first order; this is a complex issue of the so-called 'random first-order transition' explored, for instance, in [27] — for us it is sufficient to simply use the empirical form (5). It has been broadly discussed in the literature that nematic elastomers of the so-called 'isotropic genesis' should have such behavior [27], in contrast to the materials of 'nematic genesis' – where the uniaxial internal stress is frozen into the order and the resulting order parameter $Q(T)$ is supercritical [28]. Figure 1(a) shows the two characteristic types of the order parameter variation, taken from the literature; in the rest of this paper we shall be working with the form of Eq. (5) with understanding that in some practical systems the singularity at $T = T_c$ would be smoothed out.

The order parameter can be related to the impurity concentration, $\phi_{\rm imp}$, as T_c decreases linearly with impurity concentration [13, 29],

$$T_{\rm c} = T_0(1 - \beta\phi_{\rm imp}), \qquad (6)$$

where β is a constant (of the order 0.1 [13]). In this work, we use $Q_0 = 0.5$, with $T = 300$ and $T_0 = 320$ for the parametrization, so that the experimentally measured $Q(T)$ in a typical nematic elastomer is approximately reproduced. This relation explains how adding impurities changes the shape of the LCEs. We assume these parameters to be independent of other variables, since we assume that the phase transition is the property of the mesogenic units in the LCE network (i.e. the cross-linking does not affect the phase transition in the first approximation). If the impurity/solvent concentration is kept constant, stretching does not change the volume and so would not affect the mesogens, hence, λ should not affect the parameters in Eq. (6).

Figure 1(b) shows the resulting dependence of the nematic order parameter Q on $\phi_{\rm imp}$, while Fig. 2 illustrates the associated spontaneous extension along the director obtained from Eqs. (4) and (7). In particular, we see in Fig. 2(b) that the sample length decreases as the impurity concentration increases, suppressing the nematic order in the material.

The same scenario applies for a swollen nematic gel: one could manipulate the order parameter and the shape of the gel by changing the solvent concentration. In the rest of this paper we interpret the solvent swelling the polymer network as the impurity, i.e. $\phi_{\rm imp} = \phi$. However, for the gel, the conservation of the volume occupied by the network does not apply if the solvent concentration changes. Instead, we have $\lambda_x\lambda_y\lambda_z = 1/(1-\phi)$, where ϕ is the solvent volume fraction. The formula for the spontaneous extension, λ_m, in (4) has to be modified accordingly:

$$\lambda_m = \left(\frac{l_{\parallel} l_{\perp 0}}{(1-\phi) l_{\parallel 0} l_{\perp}}\right)^{1/3}. \qquad (7)$$

In the isotropic phase the length along the (former) director increases affinely with the volume, as $(1-\phi)^{-1/3}$, as marked by the dashed line in the plot.

Mixing free energy

Introducing solvent to the system also adds the interaction between the solvent and the elastomer. In a good solvent, this causes the polymers to swell. The energy of mixing polymers in the solvent is given by the Flory-Huggins equation [30]

$$F_{\rm mix} = N_{\rm tot}(\phi) k_{\rm B} T \left[\frac{(1-\phi)\ln(1-\phi)}{N_{\rm p}} + \phi\ln\phi + \phi(1-\phi)\chi\right]. \qquad (8)$$

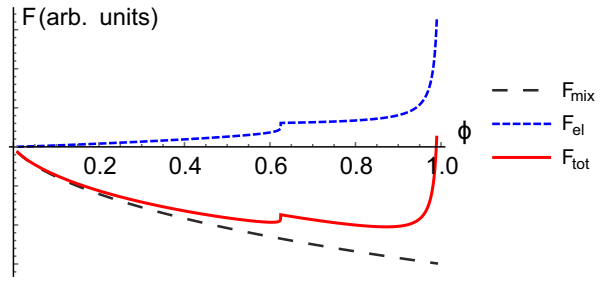

FIG. 3: [Color online] Plots of $F_{\rm el}$, $F_{\rm mix}$ and $F_{\rm tot}$ against solvent volume fraction ϕ in good solvent, for $\lambda = 1$, that is, without initial pre-stretching of the dry elastomer. The kink seen in the elastic part of the free energy is a point where the nematic order parameter drops to zero: cf. Fig. 1.

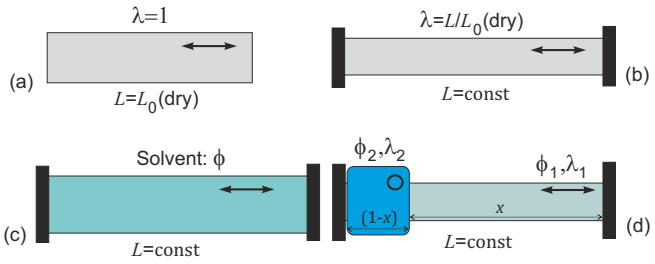

FIG. 4: [Color online] Schematic illustration of the instability: (a) aligned elastomer in stress-free equilibrium nematic state; (b) the sample stretched by extension λ along the director axis, after which the length L remains fixed; (c) the sample is swollen by adding solvent molecules with volume fraction ϕ. (d) After the instability the sample is split into two regions with different ϕ and λ, in proportion x and (1-x); the higher-ϕ portion is in the isotropic state.

Here $N_{\rm tot}(\phi) = N_{\rm s}(\phi) + N_{\rm p}$, where $N_{\rm s}$ is the number of solvent molecules. The solvent volume fraction $\phi \approx N_{\rm s}/(N_{\rm s} + N_{\rm p})$, while $1 - \phi$ gives the volume fraction of the polymer. The Flory χ parameter measures the effective solvent-polymer interaction. As $N_{\rm p}$ is very large (extensive), the first term in the brackets in $F_{\rm mix}$ can be ignored for a cross-linked network. Writing $N_{\rm tot}$ in terms of ϕ and $N_{\rm p}$, we obtain an equivalent expression:

$$F_{\rm mix} = \frac{N_{\rm p}}{1-\phi} k_B T \left[\phi \ln \phi + \phi(1-\phi)\chi\right]. \qquad (9)$$

The total free energy is then the sum of the two contributions: $F_{\rm tot} = F_{\rm el} + F_{\rm mix}$. The cross-linking ratio, ν, gives the ratio between the strength of $F_{\rm el}$ and $F_{\rm mix}$. Figure 3 shows $F_{\rm el}$, $F_{\rm tot}$ and $F_{\rm tot}$ as a function of ϕ for constant $\lambda = 1$ (no stretching) and $\nu = 0.1$. The mixing free energy decreases as more solvent is added, as expected for good solvents. However, the plot of $F_{\rm mix}$ shows a non-zero value at $\phi = 1$ as opposed to zero when the system only has one species (no mixing). This is because $N_{\rm tot}(\phi)$ depends on ϕ and goes to infinity as $\phi \to 1$ while $N_{\rm p}$ is still finite, i.e. there is still some mixing. Swelling increases the elastic free energy. There is a kink in the $F_{\rm el}$ curve due to the phase transition to the isotropic phase at higher solvent concentration. The minimum in $F_{\rm tot}$ corresponds to the optimum swelling of the gel.

III. BISTABILITY AND OPTIMUM SWELLING

Figure 4 shows schematically how we model the instability. Initially, the elastomer is in the dry state with length L_0 (a). This will be the reference state ($\lambda = 1$). Then, we stretch the elastomer to a fixed length, L, with a stretching ratio $\lambda = L/L_0 =$ constant (b). Solvent molecules are added to the system. The elastomer swells to an optimum swelling with solvent volume fraction ϕ (c). This is the homogeneous swollen nematic state. The instability occurs and the homogeneous state splits into two different states (d). The last step will be discussed in section IV. We need to be able to calculate the free energy at each state of the instability. Having combined the elasticity and mixing free energy, we looked at how the total free energy varies as a function of parameters.

The shape of the total free energy curve depends on the parameter χ. For a solvent with a large positive value of χ, the total free energy has the absolute minimum within the nematic range (upper curve in Figure 5(a)). On the other hand, a very good solvent, χ very negative, can have the minimum at large ϕ, within the isotropic range (lower curve in Figure 5(a)). The kink near the phase boundary gives rise to two minima, one in the nematic region and another in the isotropic region. This is bistability and it allows the system to split into two phases. Figure 5(a) shows $F_{\rm tot}$ for different values of χ. For large χ, i.e. poor or not very good solvents, only one minimum exists. However, the second minimum develops as χ is lowered. This means there is a bistability for a very good solvent.

We wanted to analyze the evolution of the bistability as a function of χ. The second minimum exists when the gradient at $\phi_{\rm c}$, the concentration at which phase transition occurs, becomes negative. This happens when χ is smaller than $\chi_{\rm c}$. Figure 6 shows $\chi_{\rm c}$ as a function of extension, λ. The plot shows that the bistability always exists for good solvents. This depends on the choice of parameters, such as the parametrization of the order parameter in (5), and the cross-linking ratio, ν. The plot also shows that stretching promotes bistability as $\chi_{\rm c}$ increases as the extension is larger. The value of $\chi_{\rm c}$ can be calculated as a function of parameters:

$$\chi_{\rm c} = -\frac{(1 - Q[\phi = 0])\nu/\lambda + 1 - \phi_{\rm c} + \ln(\phi_{\rm c})}{(1-\phi_{\rm c})^2}. \qquad (10)$$

Next, we calculated the free energy for different stretching to see how the minima evolve as a function of extension. We used $\chi = 0$, which is below $\chi_{\rm c}$ so that there is bistability. Figure 5(b) shows how the free en-

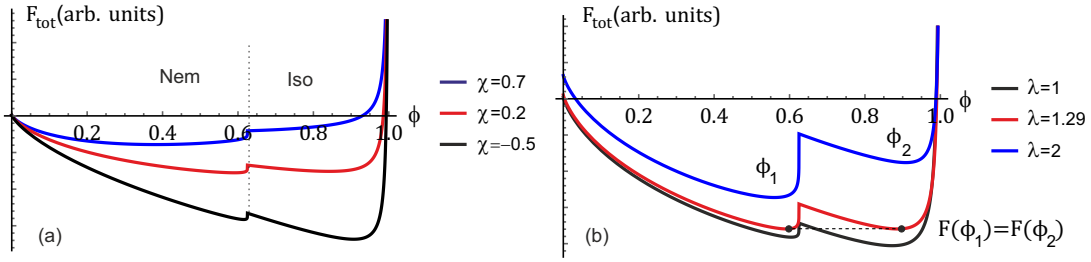

FIG. 5: [Color online] (a) Plot of $F_{\rm tot}$ against ϕ for different values of χ, at $\lambda = 1$ (i.e. without initial pre-stretching of the dry elastomer). Lower values of χ mean better solvent quality and stronger natural swelling. The step, also seen in Fig. 3, is a point where the nematic phase turns isotropic with an apparent singularity: cf. Fig. 1. (b) Plot of $F_{\rm tot}$ against ϕ for different values of λ with $\chi = 0$. ϕ_1 and ϕ_2 are the values of ϕ at the nematic and isotropic minima, respectively. Dash line denotes when the free energy values are equal at the two minima (which we denote $\lambda_{\rm crit}$).

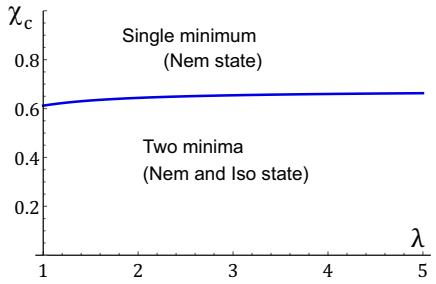

FIG. 6: Plot of $\chi_{\rm c}$, below which bistability occurs, against the imposed extension λ. Note the very weak dependence $\chi_{\rm c}(\lambda)$ over a long range of strains.

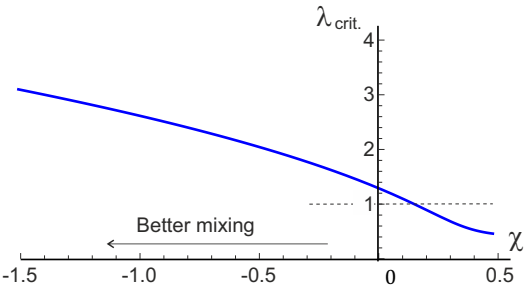

FIG. 7: Plot of $\lambda_{\rm crit}$, at which the total free energy of the nematic and isotropic states are equal, against mixing parameter χ. The dashed line marks the non-stretched state (λ=1), corresponding to Fig. 5(a).

ergy at the two minima, $F_{\rm tot}(\phi_1)$ and $F_{\rm tot}(\phi_2)$, changes as λ increases. At $\lambda = 1$, we have $F_{\rm tot}(\phi_1) > F_{\rm tot}(\phi_2)$. This means the isotropic state is more stable than the nematic state, with an energy barrier between them. As λ is increased, $F_{\rm tot}(\phi_1)$ becomes closer to $F_{\rm tot}(\phi_2)$. $F_{\rm tot}(\phi_1) = F_{\rm tot}(\phi_2)$ when λ is at $\lambda_{\rm crit} = 1.29$. Above $\lambda_{\rm crit}$, $F_{\rm tot}(\phi_1) < F_{\rm tot}(\phi_2)$, i.e. the nematic state becomes more stable. This is expected because stretching would promote ordering along the stretching direction. The energy barrier between them is also larger as λ is increased. Figure 7 shows $\lambda_{\rm crit}$ as a function of χ. The nematic state becomes less stable as the the mixing is better. This is because a better solvent gives a larger swelling.

We see that under right conditions, the bistability exists in the system with two minima at the nematic (low ϕ_1) and isotropic (high ϕ_2) states. This predicts the fiber splitting into solvent-rich isotropic, and solvent-poor nematic regions that was sketched in Figure 4. The pocket at the middle of the fibre is at the isotropic minimum, whereas the rest is at the nematic minimum. The concentrations at each minimum can be determined from the minima of the plots in Figure 5. We also see that stretching has an effect on the relative stability of the two states. In general, stretching the elastomer decreases the amount of solvent for the nematic state while increases the swelling for the isotropic state (in agreement with [19]). The optimum swelling of the homogeneous swollen nematic state, i.e. Figure 4(c) in our model, would take the value of ϕ_1. With these calculation, we can now find the energy cost of the swelling instability.

IV. SWELLING INSTABILITY

We model the instability by splitting the elastomer into two regions, each with different homogeneous swelling and stretching, Figure 4(d). The position of the isotropic pocket is irrelevant to our calculation. Region I (nematic state) has solvent volume fraction ϕ_1 and extension λ_1, whereas region II is isotropic, with ϕ_2 and λ_2. We define the molar fractions of the region I and II to be x and $1 - x$, respectively.

In equilibrium the chemical potential of solvent inside the elastomer in each region has to be equal the chemical potential of the pure solvents outside. In addition, the values of ϕ_1 and ϕ_2 minimize the total free energy in each region, producing the combined condition:

$$\left.\frac{\partial F_{\rm total}(\phi,\lambda_1)}{\partial\phi}\right|_{\phi=\phi_1} = \left.\frac{\partial F_{\rm total}(\phi,\lambda_2)}{\partial\phi}\right|_{\phi=\phi_2} = 0. \quad (11)$$

As a result, they depend on λ_1 and λ_2. To find the values

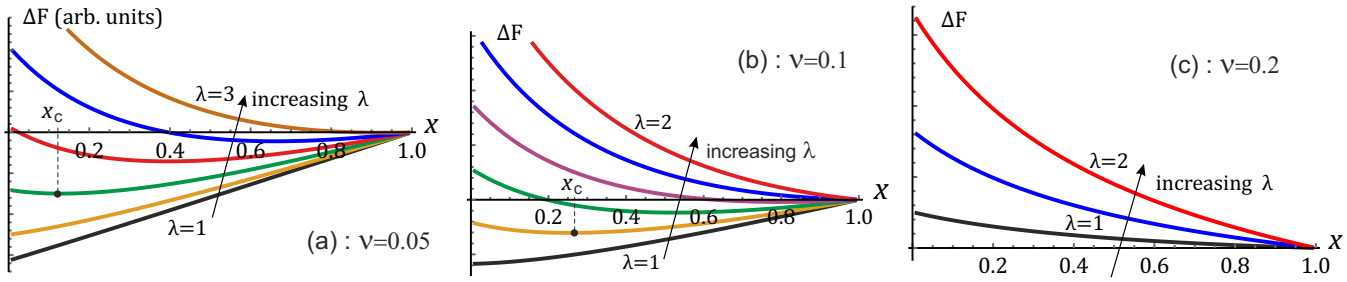

FIG. 8: [Color online] The energy cost for the instability, ΔF, as a function of separation fraction x for different stretching λ. The three plots are for an increasing cross-linking density of elastomer network (see below): (a) $\nu = 0.5$, i.e. about 20 monomers between cross-links, (b) $\nu = 0.1$, about 10 monomers, and (c) $\nu = 0.2$, i.e. every 5th monomer is cross-linked. The minima of curves denote the optimum molar fraction of the separation x_c.

λ_1 and λ_2, we need to consider balancing of the force at the junction between the two regions. The force along the elastomer is given by

$$f_i = \frac{1}{L_{i0}} \frac{\partial F_{\rm tot}}{\partial \lambda_i}, \tag{12}$$

where f_i is the force along the i direction, L_{i0} is the initial length along the i direction and λ_i is the stretching ratio along the i direction. The total length must be fixed and so this imposes another constraint,

$$x\lambda_1 + (1-x)\lambda_2 = \lambda. \tag{13}$$

Both $F_{\rm tot}$ and L_{i0} scale with the number of monomers in the elastomer. This means the force is intensive and the different size of L_{i0} and $N_{\rm x}$ in $F_{\rm tot}$ for each region can be ignored when calculating the force. Balancing the force along the stretching axis gives

$$\frac{\partial F_{\rm tot}(\phi_1, \lambda_1)}{\partial \lambda_1} = \frac{\partial F_{\rm tot}(\phi_2, \lambda_2)}{\partial \lambda_2}. \tag{14}$$

By solving (11), (13) and (14) together, we obtain λ_1 and λ_2 as a function of x. The instability occurs if it lowers the total free energy. We calculated the change in the total free energy, ΔF, as the difference between a possibly inhomogeneous state with regions of sizes x and $(1-x)$ coexisting on the fiber, and the homogeneous state of stretched and swollen sample:

$$\Delta F = xF_{\rm tot}(\phi_1, \lambda_1) + (1-x)F_{\rm tot}(\phi_2, \lambda_2) - F_{\rm tot}(\phi, \lambda). \tag{15}$$

Figure 8(b) shows the plot of ΔF against x, using the same parameters as in the previous section. The instability can occur if $\Delta F < 0$. The optimum value of x, defined as x_c, can be calculated by minimizing ΔF with respect to x. For small stretching, $x_c = 0$ and the elastomer becomes homogeneously isotropic. On the other hand, $x_c = 1$ for large stretching and the elastomer remains homogeneous. At intermediate values of λ, x_c takes a value between 0 and 1. Figure 9(a) shows that the value of x_c increases linearly with λ up to $x_c = 1$. This means we have the separation at these values of λ, with the

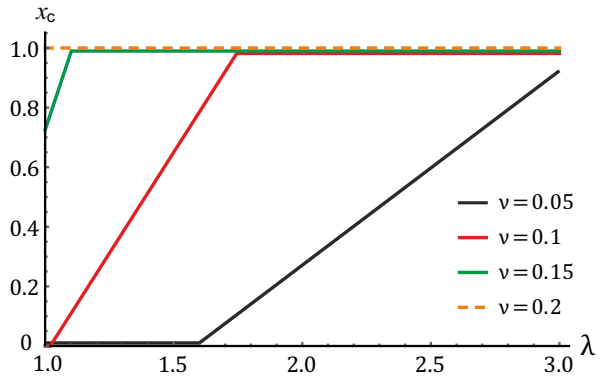

FIG. 9: [Color online] Plot of x_c as a function of λ for different cross-linking ratios ν. When $x_c \neq 1$ or 0, the fiber is split into two distinct coexisting regions as shown in Fig. 4(d). The pure states: $x_c = 0$ implies the homogeneous isotropic state; $x_c = 1$ implies the homogeneous nematic state. It appears the 10% crosslinking density is the 'best' case to observe the coexistence and swelling instability.

isotropic pocket getting smaller as the elastomer is being stretched. The fractional length of each region can be calculated from the values of x_c, and the extensions λ_1 and λ_2 at x_c as:

$$\frac{L_1}{L} = \frac{x_c\lambda_1(x_c)}{\lambda} \quad \text{and} \quad \frac{L_2}{L} = \frac{(1-x_c)\lambda_2(x_c)}{\lambda}, \tag{16}$$

where L_1 and L_2 are the lengths of the nematic and isotropic regions respectively.

Another factor that we need to consider is the cross-linking ratio ν. Increasing the ratio enhances the effect of elasticity over the mixing interaction. We expect high swelling for small ν, which increases the propensity of the isotropic state. In contrast, large ν should give poor mixing and promotes the nematic state with smaller swelling. Figure 8 shows ΔF as a function of x with $\nu = 0.05$ (a) and 0.1 (b), which are in contrast with the case of $\nu = 0.2$ in (c). For the low and medium cross-linking density, $\nu = 0.05$ and 0.1, at low stretching state with small x is preferable compared to the case of $\nu = 0.1$. This is

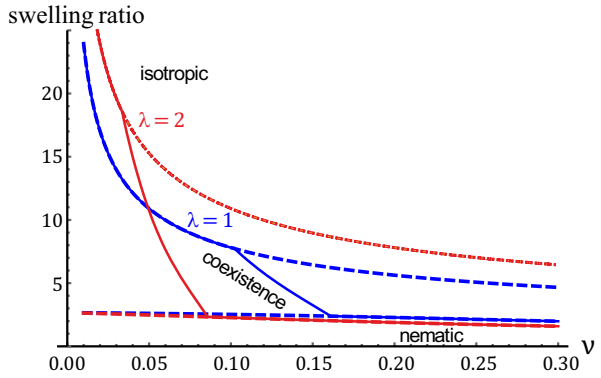

FIG. 10: [Color online] The overall swelling ratio of the sample as a function of cross-linking ratio ν for the imposed strain $\lambda = 1$ (no stretching) and $\lambda = 2$. Dashed lines show the swelling ratio if the elastomer remained in the homogeneous isotropic/nematic state, respectively.

because isotropic state has relatively lower energy and larger stretching is required to obtain $x_c \to 1$. Figure 9 shows x_c as a function of λ for different values of ν. For the highly cross-linked elastomer, $\nu = 0.2$, only $x = 1$ is energetically favorable, i.e., the elastomer can only be entirely nematic. This shows that stronger cross-linking prevents the instability from occurring at any extension.

This is summarized in Figure 10. The plot shows the commonly used characteristic of gels: the swelling ratio (defined as {swollen volume}/{dry volume}) as a function of ν. The plot shows highly swollen isotropic at small ν and smaller swollen nematic state at large ν. Intermediate values give coexistence between the two states, i.e. splitting of the elastomer, with the average swelling ratio between the values of the isotropic and the nematic states. We see that the instability cannot occurs at high cross-linking regime. Stretching the elastomer would lower the values of ν corresponding to the transitions.

V. CONCLUSION

We have shown that the shape instability could lower the total free energy of the system where the swelling in a good solvent competes with the nematic elasticity response to an imposed stretching. The conditions and the size of the instability can be calculated for different amount of stretching of the elastomer sample. We found that a nematic elastomer in a good solvent exhibits bistability, allowing the swollen network to separate into two phases. An isotropic pocket could be formed along the sample where most of the solvent will accumulate, its size depends on the stretching as well as the degree of cross-linking of the network. In general, stretching promotes nematic ordering and hence decreases the size of the isotropic pocket formed in the instability. More crosslinks in the network also favor nematic ordering and inhibit the instability. This will be useful for utilizing nematic elastomer filament in actuator applications.

However, the model that we presented here cannot predict the shape of the highly swollen isotropic pocket. A more realistic (and much more complicated) theory would include the energy penalty for a sharp inhomogeneous interface between the different regions, i.e. including the gradient terms in the free energy of a nematic elastomer [31]. Another simplification that we imposed was to treat the order parameter, Q, as an experimentally prescribed function of solvent concentration and temperature. This allowed a lot of progress to be made, however, a more rigorous way is to add the thermodynamic free energy of the order parameter and treat Q as another independent variable.

Acknowledgments

This work has been carried out as part of the Cavendish Masters programme in Physics, and supported by the EPSRC Critical Mass grant for Theoretical Condensed Matter. We are grateful to Profs. M.H. Godinho and P. Pieranski for attracting out attention to this problem via their beautiful experiments on swelling of cellulosic fibers, and to Prof. M. Warner for support and the critique of our ideas and methods.

[1] P. G. de Gennes, C. R. Acad. Sci. B **281**, 101 (1975).
[2] M. Warner, K. P. Gelling, and T. A. Vilgis, J. Chem. Phys. **88**, 4008 (1988).
[3] S. S. Abramchuk and A. R. Khokhlov, Dokl. Akad. Nauk USSR **297**, 385 (1988).
[4] J. Kupfer and H. Finkelmann, Makromol. Chem. Rapid Comm. **12**, 717 (1991).
[5] A. R. Tajbakhsh and E. M. Terentjev, Eur. Phys. J. E **6**, 181 (2001).
[6] P. M. Hogan, A. R. Tajbakhsh, and E. M. Terentjev, Phys. Rev. E **65**, 041720 (2002).
[7] K. Urayama, Macromolecules **40**, 2277 (2007).
[8] E. M. Terentjev, J. Phys.: Condens. Matter **11**, R239 (1999).
[9] P. Cicuta, A. R. Tajbakhsh, and E. M. Terentjev, Phys. Rev. E **65**, 051704 (2002).
[10] S. V. Ahir, A. R. Tajbakhsh, and E. M. Terentjev, Adv. Func. Mater. **16**, 556 (2006).

[11] T. Ikeda, S. Horiuchi, D. B. Karanjit, S. Kurihara, and S. Tazuke, Macromolecules **23**, 42 (1990).
[12] J. E. Marshall, Y. Ji, N. Torras, K. Zinoviev, and E. M. Terentjev, Soft Matter **8**, 1570 (2012).
[13] V. Anderson, E. Terentjev, S. Meeker, J. Crain, and W. Poon, Eur. Phys. J. E **4**, 11 (2001).
[14] S. V. Fridrikh and E. M. Terentjev, Phys. Rev. E **60**, 1847 (1999).
[15] S. Krause, R. Dersch, J. H. Wendorff, and H. Finkelmann, Macromol. Rapid Comm. **28**, 2062 (2007).
[16] J. Hu, S. Chen, and Q. Pan, U.S. Patent No. 20110049768 A1 (3 March, 2011).
[17] P. Calvert, Adv. Mater. **21**, 743 (2009).
[18] A. Gestos, P. G. Whitten, G. G. Wallace, and G. M. Spinks, Soft Matter **8**, 8082 (2012).
[19] R. H. Pritchard and E. M. Terentjev, Polymer **54**, 6954 (2013).
[20] M. Warner and X. J. Wang, Macromolecules **25**, 445 (1992).
[21] A. Matsuyama and T. Kato, J. Chem. Phys. **114**, 3817 (2001).
[22] P. Bladon, M. Warner, and E. M. Terentjev, Macromolecules **27**, 7067 (1994).
[23] J. M. F. Gunn and M. Warner, Phys. Rev. Lett. **58**, 393 (1987).
[24] P. Bladon, E. M. Terentjev, and M. Warner, J. Phys. II Fr. **4**, 75 (1994).
[25] M. Warner and E. M. Terentjev, *Liquid Crystal Elastomers*, Oxford University Press, 2003.
[26] S. M. Clarke, A. R. Tajbakhsh, E. M. Terentjev, and M. Warner, Phys. Rev. Lett. **86**, 4044 (2001).
[27] G. Feio, J. L. Figueirinhas, A. R. Tajbakhsh, and E. M. Terentjev, Phys. Rev. B **78**, 020201 (2008).
[28] A. Lebar et al., Phys. Rev. Lett. **94**, 197801 (2005).
[29] K. P. Sigdel and G. S. Iannacchione, J. Chem. Phys. **133**, 044513 (2010).
[30] J. R. Fried, *Polymer Science and Technology*, Pearson Education, 2nd edition, 2003.
[31] E. M. Terentjev, M. Warner, and G. Verwey, J. Phys. II **6**, 1049 (1996).